Unraveling proteoform complexity by native liquid chromatography-mass spectrometry

Schaick, G. van

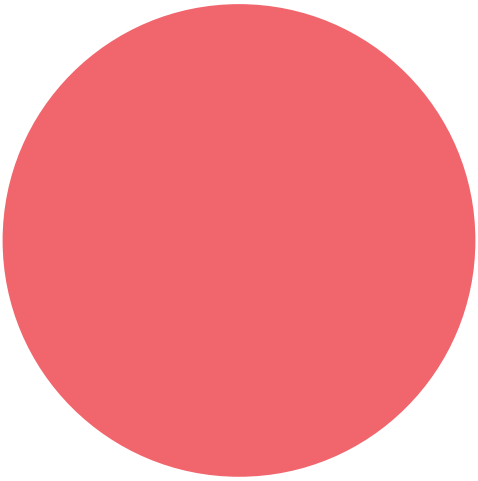

5

Online collision-induced unfolding of therapeutic monoclonal antibody glyco-variants through direct hyphenation of cation exchange chromatography with native IM-MS

G. van Schaick [1], E. Domínguez-Vega [1], J. Castel [2,3], M. Wuhrer [1], O. Hernandez-Alba [2,3], S. Cianférani [2,3]

[1] Center for Proteomics and Metabolomics, Leiden University Medical Center, Leiden, the Netherlands

[2] Laboratoire de Spectrométrie de Masse BioOrganique, IPHC UMR 7178, Université de Strasbourg, CNRS, Strasbourg, France.

[3] Infrastructure Nationale de Protéomique ProFI, FR2048 CNRS CEA, Strasbourg, France.

Manuscript submitted

Post-translational modifications (PTMs) not only substantially increase structural heterogeneity of proteins but can also alter the conformation or even biological function. Monitoring of these PTMs is particularly important for therapeutic products, including monoclonal antibodies (mAbs), since their efficacy and safety may depend on the PTM profile. Innovative analytical strategies should be developed to map these PTMs as well as explore possible induced conformational changes. Cation exchange chromatography (CEX) coupled to native mass spectrometry (nMS) has already emerged as valuable asset for the characterization of mAb charge variants. Nevertheless, questions regarding protein conformation cannot be explored using this approach. Thus, we have combined CEX separation with collision induced unfolding (CIU) experiments to monitor the unfolding pattern of separated mAbs and thereby, pick up subtle conformational differences without impairing the CEX resolution. Using this novel strategy, only four CEX-CIU runs had to be recorded for a complete CIU fingerprint either at the intact mAb level or after enzymatic digestion at the mAb subunit level. As proof-of-concept, CEX-CIU was first used for an isobaric-mAb mixture to highlight the possibility to acquire individual CIU fingerprints of CEX-separated species without compromising CEX separation performances. CEX-CIU was next successfully applied to mAb glyco-variants conformational characterization, in order to derive glycoform-specific information on the gas-phase unfolding, CIU patterns of Fc fragments revealing increased resistance of sialylated glycoforms against gas-phase unfolding. Altogether, we demonstrated the possibilities and benefits of combining CEX with CIU for in-depth characterization of mAb glycoforms, paving the way for linking conformational changes and resistance to gas-phase unfolding charge variants.

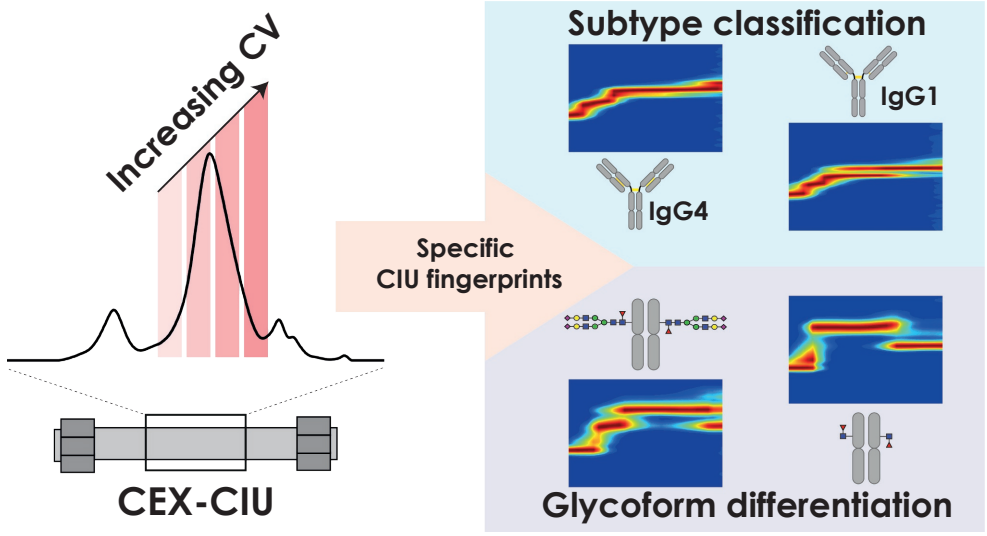

5.1 Introduction

Monoclonal antibodies (mAbs) have taken a dominant role in the treatment of various disorders [4, 12] and this class of human therapeutics is still rapidly expanding. Currently, most therapeutic mAbs are IgG1 subclass, but other IgG subclass formats are also being produced (IgG2 or IgG4) [247]. Besides variation in subclass, therapeutic mAbs can contain a plethora of different post-translational modifications (PTMs), including lysine clipping, pyroglutamate formation, glycosylation, oxidation and deamidation [115, 248]. Changes in PTM profile may influence the conformation and thereby, impact biological function (i.e., efficacy and safety of therapeutic proteins). For instance, mAb charge variants, such as deamidated species and proteoforms with isomerization of asparagine residues, may result in decreased binding affinity and potency [249]. Novel strategies are needed to fully characterize charge-related structural changes to ensure efficacious and safe therapeutic products.

Over the last decades, cation exchange chromatography (CEX) coupled to UV detection has found its way into quality control as reference technique to monitor charge variant profiles of mAb-based therapeutic products [82, 161]. Nevertheless, these robust and routinely-used methods often lack the ability to perform in-depth structural characterization without time-consuming fraction collection followed by offline mass spectrometry (MS). Fortunately, recent advances dealing with interfacing CEX and native MS (nMS) enabled the development of methodologies providing online separation, identification and characterization of charge variants [217]. Most importantly, the replacement of traditional non-volatile salt gradients with low ionic strength pH gradients using (MS-compatible) ammonium-based mobile phases boosted the application of CEX-nMS for charge variants analysis [102, 115, 250]. While these pH gradients already result in sufficient separation efficiency for most proteins, proteins with high isoelectric points (pIs) or heterogeneous proteins consisting of many proteoforms may benefit from a pH gradient accompanied by a (minor) increase in salt concentration, so-called salt-mediated pH gradient [102, 251]. Especially the latter enabled online identification of mAb proteoforms with altered pI, such as proteoforms with differences in glycosylation, deamidation, and isomerization [159, 161, 252]. Currently. CEX-nMS applications focus largely on structural characterization of charge variants, while their effect on protein conformation or gas-phase unfolding pattern is not explored.

To decipher the conformational landscape of mAbs, ion mobility (IM)-based technologies are particularly suitable [253]. The availability of traveling wave IM

spectrometry (TWIMS) in commercial MS instruments opened many possibilities to study global protein conformation in the gas-phase [254]. Unfortunately, IM-MS measurements have often low resolving power for species with related conformations. As a consequence, the collision cross sections (CCSs) obtained from these measurements are often not very informative for intact mAb analysis [247, 255]. To circumvent this poor resolution as well as gain deeper insights into the gas-phase behavior after activation, IM-based collision-induced unfolding (CIU) has been proposed as a suitable alternative. So far, CIU has been employed to investigate different properties and modifications of mAbs [247, 255-257] and antibody-drug conjugates (ADC) [135, 150]. While these classical CIU approaches face various practical challenges preventing routine use, including manual buffer exchange and time-consuming data acquisition process, online coupling of size exclusion chromatography (SEC) with CIU allowed automation of this workflow tackling these challenges [134].

Here, we present an innovative online CEX-CIU method for the in-depth characterization of mAb populations in their native state in a fast and straightforward manner. Using this approach, mAb populations were separated according to their pI and their specific unfolding patterns were acquired by increasing the collision voltage in the trap cell prior to IM separation during the elution of the selected mAb population. This analytical strategy was developed to record the CIU fingerprints of intact or IdeS-digested mAbs showing the capability of this technique to generate CIU fingerprints of CEX-separated protein populations. Subsequently, CEX-CIU hyphenation was tailored to decipher conformational differences of an equimolar mixture of three nearly isobaric mAbs. Finally, the potential of CEX-CIU for charge variant analysis is illustrated by studying gas-phase unfolding resistance of different remodeled glycan-variants of a reference mAb.

5.2 Experimental section

5.2.1 Materials

Eculizumab (Soliris, Alexion), trastuzumab (Herceptin, Roche), pembrolizumab (Keytruda, Merck) were obtained from their manufacturers. The glycan-remodeling was performed by treatment of trastuzumab with TransGLYCIT (Genovis, Lund, Sweden) according to the producer specifications with and without the presence of a fucosidase. For middle-level analysis, enzymatic digestion was performed by incubation of one unit of IdeS enzyme (FabRICATOR, Genovis, Lund, Sweden) per microgram of mAb at 37 °C for 60 min. Prior to further analysis, the samples were buffer exchanged to 50 mM ammonium acetate using 10 kDa Vivaspin 500 filters (Sartorius, Göttingen,

Germany) with an end concentration 2 mg/ml.

5.2.2 CEX separation

The CEX measurements were performed using an Acquity UPLC H-class system (Waters, Wilmslow, UK) equipped with quaternary solvent manager, sample manager operated at 10 °C, column oven and TUV detector. A BioResolve SCX column (2.1 x 100 mm, 3µm) was used from Waters. The mobile phases were composed of 50 mM ammonium acetate at pH 5.0 (A) and 160 mM ammonium acetate at pH 8.6 (B). For the intact trastuzumab, a linear gradient from 50 to 70% B in 10 min was applied. The middle-level trastuzumab separation was achieved by a linear gradient from 30 to 70% B in 10 min. The mixture of mAbs was separated by first maintaining 0% B for 1 min followed by a linear gradient from 30 to 70% B in 9 min. All CEX methods contained a column cleaning step at 100% B for 3 min and re-equilibration step at 0% B for 7 min. The injected amount of intact mAbs was 20 µg and middle-level mAbs was 12 µg. The flow rate was 0.1 ml/min and the UV wavelengths were 280 and 214 nm.

5.2.3 CEX-ESI-CIU experiments

CEX was coupled online to a Synapt G2 HDMS mass spectrometer (Waters) operated in positive mode with a capillary voltage of 3 kV and sample cone voltage of 180 V. The backing pressure of the Z-Spray source was increased to 6 mbar. Desolvation and source temperatures were set to 450 and 90 °C, respectively. Desolvation and cone gas flow rates were 750 and 60 l/h, respectively. The cone voltage of the Synapt G2 was lowered to 80 V (for intact analysis) or 60 V (for middle-level analysis). The argon flow rate was set to 2 ml/min. Prior to the IM cell, ions were focused in the helium cell (120 ml/min). In the IM cell, the N_2 flow of 60 ml/min was applied and the wave height and velocity were 40 V and 800 m/s. Other settings were similar as mentioned for the CEX-nMS analysis. The *m/z* range was from 1000 to 10,000. External calibration was performed using cesium iodide (2 mg/ml in 50% isopropanol).

For the CEX-CIU experiments, the collision voltage (CV) in the trap cell was stepwise increased from 0 to 150 V (steps of 10 V). One complete CIU fingerprint was obtained in four CEX runs, where each CEX run contained four IM-MS functions per selected species (0-30 V, 40-70 V, 80-110 V, and 120-150 V). For each of these voltage steps, the number of scans and scan time were 4 and 0.2 min, respectively. The start and end time of the functions was adjusted to the retention time of the species of interest and between the functions during elution, 0.5 s was kept ensuring effective application and stable CVs.

5.2.4 ESI-CIU experiments

Intact or middle-level trastuzumab was infused in an ESI source using a syringe pump (KD Scientific, Holliston, MA, USA) with 250 µL syringe (Hamilton, Bonaduz, Switzerland) at a rate of 3 µl/min. The parameters of the Synapt G2 were as described for CEX-CIU experiments. The CVs in the trap cell were manually increased from 0 to 150 V in steps of 10 V and from each CV, 0.5 min was acquired.

5.2.5 Data analysis

The CEX-IM-nMS data was processed with MassLynx (v4.1) and data from CIU experiments was analyzed and visualized using CIUSuite2 (v2.2) [258] or ORIGAMI^{ANALYSE} (v1.2.1.6) [259]. The chromatographic resolution was calculated with $R_s = 1.18*((t_{R2} - t_{R1})/(W_{FWMH1} + W_{FWMH2}))$, where t_r is the retention time in min and W_{FWMH} is the peak width at half height in min. The drift times obtained with CEX-IM-nMS were converted into CCS values using external calibrants, including β-lactoglobulin and concanavalin A for the middle-level and concanavalin A, alcohol dehydrogenase and pyruvate kinase on the intact level [260]. Arrival time distributions (ATDs) were smoothed with the Savitzky-Golay algorithm with window length of 5 and polynomial order of 2. The data was interpolated with factor of 2 on the CV axis. For all CIU analyses, averaged and differential plots, including root-mean square deviation (RMSD) values, were obtained. Feature detection and CIU50 analysis were performed using standard mode, where minimum feature length was 2 steps, feature allowed width was 0.75 ms, no CV gap length within a feature was allowed, drift time spectrum was centroid at the maximum value for each CV, and transition region padding was 15 V. The univariate feature selection (UFS) plots were generated to highlight diagnostic voltages (i.e., high -log10(p-value) scores) to classify mAb subclasses.

5.3 Results and discussion

5.3.1 CEX for mAb charge variant separation at intact and middle level

According to the separation capabilities of CEX for therapeutic mAbs, we implemented two different CEX-nMS methods to monitor charge variants of a reference mAb (trastuzumab) at both intact and middle level. Most efficient separation of charge variants of trastuzumab was achieved using a salt-mediated pH gradient with mobile phases composed of 50 mM ammonium acetate at pH 5.0 (A) and 160 mM ammonium acetate at pH 8.6 (B). Applying these mobile phases with a gradient from 50 to 70% B, we resolved acidic and basic species from the main form of intact trastuzumab (**Fig. 1a**) with similar separation efficiencies as previously reported [102, 250]. The

main form of trastuzumab eluted at 13.6 min with a full width at half maximum (FWHM) of 0.77 min. Besides this form, additional acidic and basic variants were separated, which could be assigned based on previous (bottom-up) data [102, 159, 250, 261]. The acidic species, including deamidated variants, eluted at 11.9 min and were baseline resolved from the main peak (resolution 1.6). Basic charge variants due to isomerization of Asp residues eluted later at 14.9 min (resolution of 1.2) (**Fig. 1a, Table S1**).

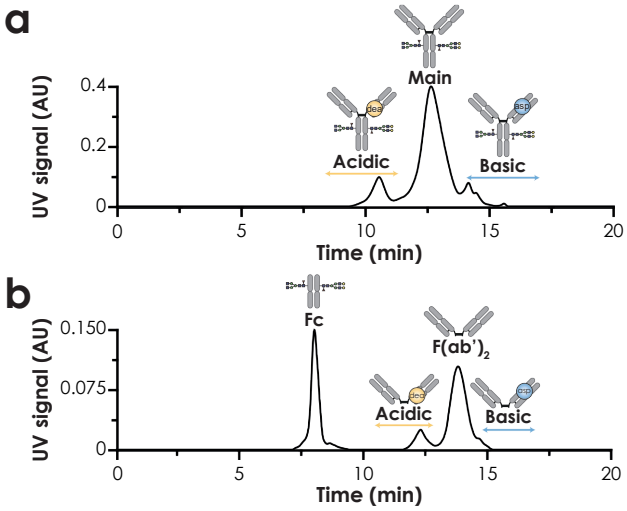

Figure 1 | CEX-UV chromatograms of intact trastuzumab (**a**) and middle-level analysis of trastuzumab (**b**). For intact trastuzumab, acidic (deamidated proteoforms) and basic species (IsoAsp variants) were separated. The middle-level analysis resulted in two main peaks corresponding to the Fc and $F(ab')_2$ fragments. Similar charge variants as for intact trastuzumab were observed on $F(ab')_2$ part.

Although analysis of intact mAbs can be very informative, CEX-nMS on mAb subunits upon IdeS digestion [262] (i.e., cleavage of mAb below hinge region) allowed localization of charge variants at the subunit level along with more precise mass measurements facilitating PTM identification [255] (**Fig. 1b**). The CEX separation of the Fc and $F(ab')_2$ fragments was accomplished using the same mobile phases with a gradient from 30 to 70% B (**Fig. 1b**; **Table S1**). While the Fc fragment eluted as a single peak at 8.0 min, multiple peaks were observed for the $F(ab')_2$ domain. Besides the main $F(ab')_2$ peak at 13.9 min, also acidic and basic species were separated at 12.3 min and 14.8 min, respectively. The latter indicated that the deamidation and isomerization occur on the $F(ab')_2$ domain, which is also consistent with published data [261, 263]. The peak width of the Fc peak was smaller, whereas the $F(ab')_2$ peak was very similar to intact trastuzumab. This is in line with expectations since low ionic strength mobile phases have been described to focus the chromatographic peaks, while higher ionic strength results in broader peaks [82]. In our case, the pH gradient starts at low ionic strength (50 mM) and increases in ionic strength with time.

5.3.2 Coupling of CEX and CIU

We then aimed at direct coupling of CEX to CIU to gain information on conformation of chromatography-resolved protein populations. Similar to our previously described SEC-CIU optimization procedure [134], all critical CIU parameters were adapted to obtain successful hyphenation of CEX and CIU, including acquisition time, magnitude and number of CV steps. The CV in the trap was increased from 0 to 150 V in steps of 10 V. The maximum collision voltage of 150 V was selected to minimize the risk of fragmentation and obtain high-quality data, while still covering the most diagnostic CIU energy range of mAbs. Furthermore, a cone voltage of 80 V was sufficient for intact mAb analysis, whereas for the middle level 60 V was chosen to prevent changes in mAb conformation (**Fig. S1**). To find the optimal number of CV scans per run and the acquisition time, the CEX peak width (around 0.80 min) as well as the spectral quality were considered. We compared the effect of four CVs per chromatographic peak (each CV was applied for 20 s during which 5 scans of 4 s were recorded) with six CVs (15 s for each CV during which 5 scans of 3 s were recorded) (**Fig. S2**). Even though the latter condition reduced the total analysis time (three 20-min CEX-CIU runs instead of four), noisy CIU features are obtained above 100 V due to lower S/N ratio. Therefore, a total of four CEX-CIU runs (0-30 V, 40-70 V, 80-110 V, and 120-150 V) were chosen to record a complete high-quality CIU fingerprint (**Fig. 2**). Importantly, the lowest voltages of the run covering the 0-30 V range should be recorded at the peak maximum due to low desolvation and trapping efficiencies at these low voltages together with low-intensity signal at the beginning of the chromatographic peak (**Fig. S3**). Compared to previously reported SEC-CIU method [134], CEX-CIU required longer analysis time to record the whole dataset from 0 to 150 V. More precisely, a complete CEX-CIU fingerprint will take 80 min (four times 20 min) compared to 15 min (three times 5 min) for SEC-CIU. However, CEX-CIU supplemented the CIU workflow with a chromatographic separation dimension rather than solely automated sample introduction in the MS instrument as for SEC-CIU, counterbalancing the longer acquisition times with improved separation power.

To benchmark our method development, we first applied the optimized CEX-CIU method to the analysis of reference mAb trastuzumab resulting in four different states within the whole CIU fingerprint. The conformational transitions between these four different states were observed at 18.2 ± 0.2 V, 34 ± 2 V, and 91 ± 3 V, respectively. One feature of this fingerprint is the coexistence of unfolding states 2 and 3 over a wide voltage range (between 40, and 120 V). This particular CIU signature has already been reported for

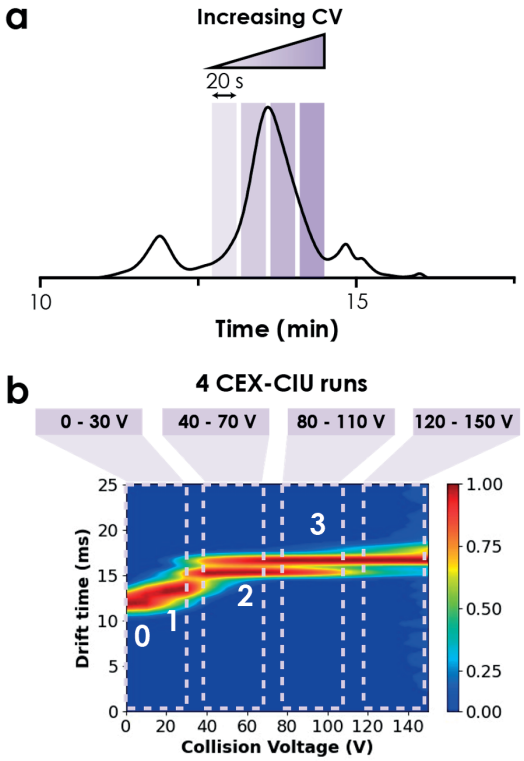

Figure 2 | CEX-CIU for mAb analysis. (**a**) CEX-UV chromatogram of intact trastuzumab showing the increase in CV to obtain the CIU fingerprint. During elution of the selected species, the CV is increased in four steps, where each CV is maintained for 20 s. (**b**) CEX-CIU fingerprint of the 27+ charge state of the trastuzumab peak indicated in the chromatogram. In total, four measurements were required to obtain a fingerprint from 0 to 150 V. The conformational states are labeled with numbers from 0 to 3. The replicate RMSD was 4.2% indicating good repeatability.

IgG1 fingerprints of high charge states (27+) [134], being in good agreement with the isotype subclass of trastuzumab. The CIU fingerprints of the CEX-separated Fc and $F(ab')_2$ domains were recorded using similar experimental parameters (**Fig. S4**). The Fc subunit (14+) showed two transitions at 27 ± 2 V and 116 ± 3 V, where the latter represented putative compaction of the subunit structure (**Fig. S4a**). To provide more insights into this latter transition, a manual inspection of the mass spectra of the Fc subunit along with the analysis of the corresponding ATD profile was performed (**Fig. S5**). According to these results, the upper limit of the Fc fingerprint was set to 130 V as further activation led to fragmentation of molecular ions and thus, to the total loss of the MS signal. As depicted in **Fig. S5**, the most unfolded state (around 12 ms) starts to be populated at 30 V and becomes the most intense conformation in the ATD at 40 V. Beyond 90 V, this conformational state starts to be less populated, favoring the increase of an additional unfolding state with shorter drift time (around 10 ms). Although further analysis should be carried out to

confirm the structural mechanism behind this conformational change, these results could suggest that the Fc subunit of mAbs can undergo compaction under specific experimental conditions. For the $F(ab')_2$ part (21+), three transitions were observed giving rise to four progressively unfolding states (**Fig. S4b**). These transitions are observed at 22.5 ± 0.1 V, 72 ± 7 V, and 128 ± 7 V, respectively.

Similar CIU fingerprints of mAbs and mAb subunits have been previously reported [134, 247, 255] indicating that the obtained CIU fingerprints of trastuzumab were not affected by the upfront CEX separation. The RMSD value between CEX-ESI-CIU and ESI-CIU at the intact level was 6.6% (**Fig. S6a**) in line with differences observed in previous studies using the combination of SEC with CIU [134]. The RMSD between the middle-level analyses using CEX-ESI-CIU and ESI-CIU was 6.5% (**Fig. S6b**). In both cases, the obtained RMSD was similar to the RMSD values between replicates (**Fig. S6**). The slightly differences observed at the intact level between inter- and intra-RMSD values can stem from the fact that both analyses were not recorded at the same flow rate (4 µl/min for ESI-CIU and 250 µl/min for CEX-ESI-CIU) along with the variation of the IM-MS signal transmission as a consequence of the chromatography peak elution when recording CIU fingerprints in combination with CEX. However, the RMSD values pinpoint that online CEX-CIU affords comparable and consistent CIU results leading to the conclusion that neither the fractionation of the CIU recording nor interaction with the CEX stationary phase significantly impair the quality of the CIU fingerprints of therapeutic mAbs.

5.3.3 Proof-of-concept: CEX-CIU for nearly-isobaric mAb mixture analysis

Since the CEX-CIU approach was shown to be well suited to monitor the unfolding mechanism of different chromatography-selected populations, this analytical strategy was applied to a mixture of three therapeutic mAbs at the intact level, as a proof-of-concept of the methodology. The proposed application can be particularly interesting for biopharmaceutical companies since the simultaneous characterization of individual components contained in a mAb mixture is gaining more attention due to novel promising co-formulated mAb products [264]. The selected mAbs belonged to different isotype subclasses exhibiting differences in inter-chain disulfide patterns. Previous studies have shown that the CIU mechanism strongly depends on the inter-chain disulfide pattern of mAbs and therefore, the CIU fingerprints of these mAbs should show different unfolding energies and number of transitions. Three therapeutic mAbs with relatively similar molecular masses but substantially different pIs (i.e., 6.1 for eculizumab, 7.6 for pembrolizumab and 9.1 for trastuzumab [265]) were chosen for the mAb mixture analysis. Thereby,

the relatively small difference in molecular masses hampered studying unfolding patterns with classical direct infusion techniques or applying non-denaturing size-based separations, such as SEC [134]. In this case, CEX-CIU would be a suitable alternative, since mAbs can be separated based on pI prior to the nMS analysis (**Table S2**). Additionally, this approach allows simultaneous detection and monitoring of minor charge variants within the mAb mixture. The CEX gradient started by maintaining 0% B for 1 min to ensure elution of eculizumab, whereafter a linear increase from 30% to 70% B in 9 min enabled separation of pembrolizumab and trastuzumab. The obtained CEX chromatogram showed three (major) distinct peaks corresponding to the different mAbs (**Fig. 3a** and **b**), where eculizumab elutes at 1.8 min, pembrolizumab at 8.9 min, and trastuzumab at 15.1 min.

After optimizing the CEX separation, the CIU fingerprints of the separated mAbs were recorded and compared (**Fig. 3c**). Using this approach, four CEX-CIU runs of 20 min (in total 80 min) were required to obtain complete CEX-CIU fingerprints for the three mAbs. A clear advantage of this approach is the low risk of interferences in the CIU pattern coming from different species since the three mAbs elute at different retention times. To illustrate the detected differences, the CIU50 values were calculated (**Fig. 3d**). In the case of trastuzumab, three different unfolding events were observed, while only two transitions were detected for eculizumab and pembrolizumab. Thereby, a CIU50 value of 95.1 ± 0.2 V was determined for this last transition (CIU50-3), being the solely mAb that undergoes unfolding transition at collision energies higher than 50 V. The RMSD between trastuzumab measured in the mixture and as single mAb was 6.1%, whereas the RSMDs between the different mAbs subclasses were ranging from 11.2% to 18.8% (**Fig. S9**). To strengthen these results, linear discriminant analysis was performed (**Fig. 3e**) showing the ability to distinguish the three mAbs based on their CIU features. This indicates that the CIU patterns of the mAbs are indeed different and no additional variation was introduced upon mixing the mAbs. Additionally, the univariate feature selection (UFS) plot pinpointed the 120-140 V region as the most diagnostic energy range to perform the inter-subclass comparison (**Fig. 3f**), being in agreement with previous reports [255, 266]. After the analysis of these results, the benefit of CEX-ESI-CIU approach is clearly shown to study a co-formulation mixture of therapeutic mAbs providing a separation of the different components in the first dimension (CEX) and subsequently recording the unfolding pattern of each protein population. The outcome of this approach not only improves the characterization of co-formulated mAbs without jeopardizing the chromatographic resolution but also reduces the overall analysis time by acquiring multiple CIU fingerprints at once.

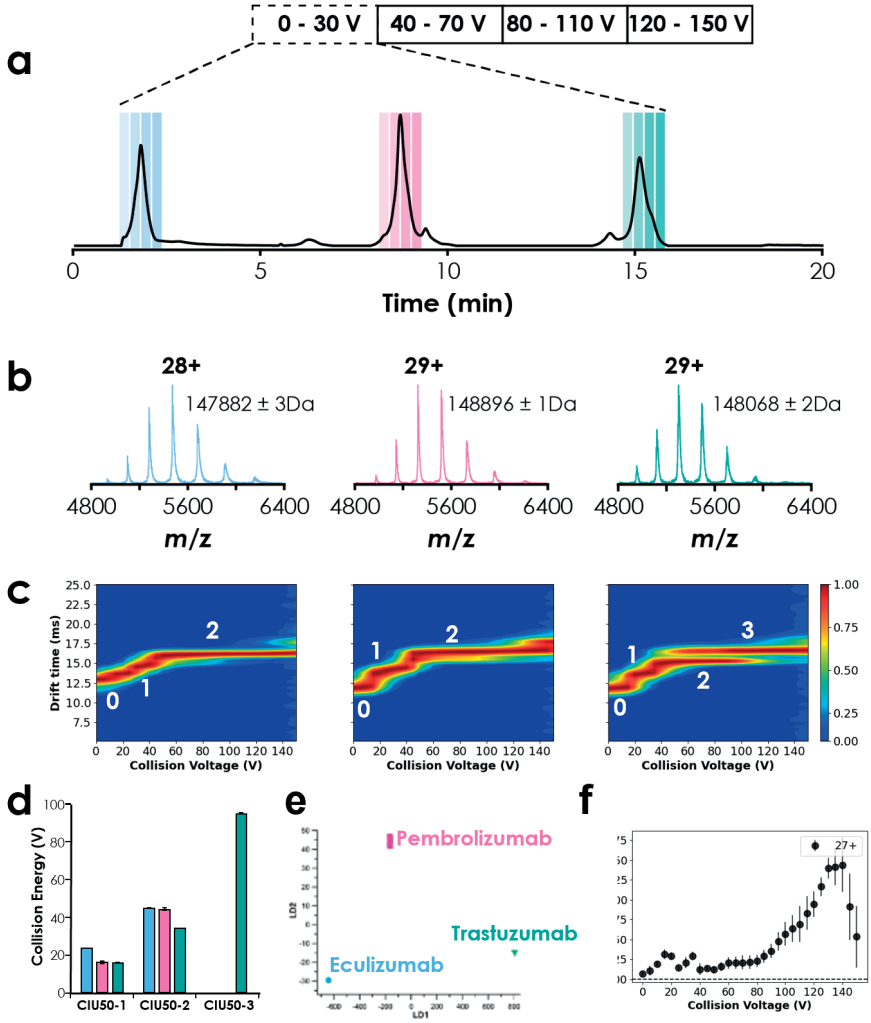

Figure 3 | CEX-CIU for multiplex analysis of different mAbs, including eculizumab (IgG2/4), pembrolizumab (IgG4) and trastuzumab (IgG1). (**a**) The CEX-UV chromatogram of mixture showing the selected peaks for CIU analysis. During elution of the selected species, the CV is increased in four steps, where each CV is maintained for 20 s. (**b**) Mass spectra of the selected CEX peaks, including the experimental mass of the most abundant species. (**c**) CEX-CIU fingerprints of the mAbs of the 27+ charge state. CEX-CIU fingerprints of the 26+ and 28+ charge state can be found in **Figure S7** and **S8**, respectively. (**d**) CIU50 values of the different detected transitions within the CIU fingerprints. (**e**) Linear determinant analysis of the three mAb CIU fingerprints. (**f**) UFS plot highlighting the critical CVs for mAb subclass identification.

5.3.4 CEX-ESI-CIU to monitor differences in gas phase unfolding of glycoforms

As previous reports have shown that glycosylation impacts the gas-phase unfolding of mAbs [256, 267], we applied the novel CEX-CIU platform to study the influence of glycosylation, particularly sialyation, on the gas-phase unfolding pattern as a particular type of charge variants.

The different glycoforms of trastuzumab were created using glycan-based enzymatic remodeling (see experimental section for details on the procedure). The heterogeneous pool of glycans present on the initial product (T0) were first partially removed (EndoS2 treatment) leading to the deglycosylated mAb (T1) followed by replacement with a particular glycoform (G2S2 with or without core F) (**Fig. 4a**). The remodeled glycans contained additional negative charges from the sialic acids, which resulted in modification of the protein surface charges. Since we were interested in differences in glycosylation located on the Fc part, the glycoengineered trastuzumab formats were digested with the IdeS enzyme and Fc and $F(ab')_2$ subunits were further analyzed by CEX-CIU. As expected, the Fc fragments with remodeled

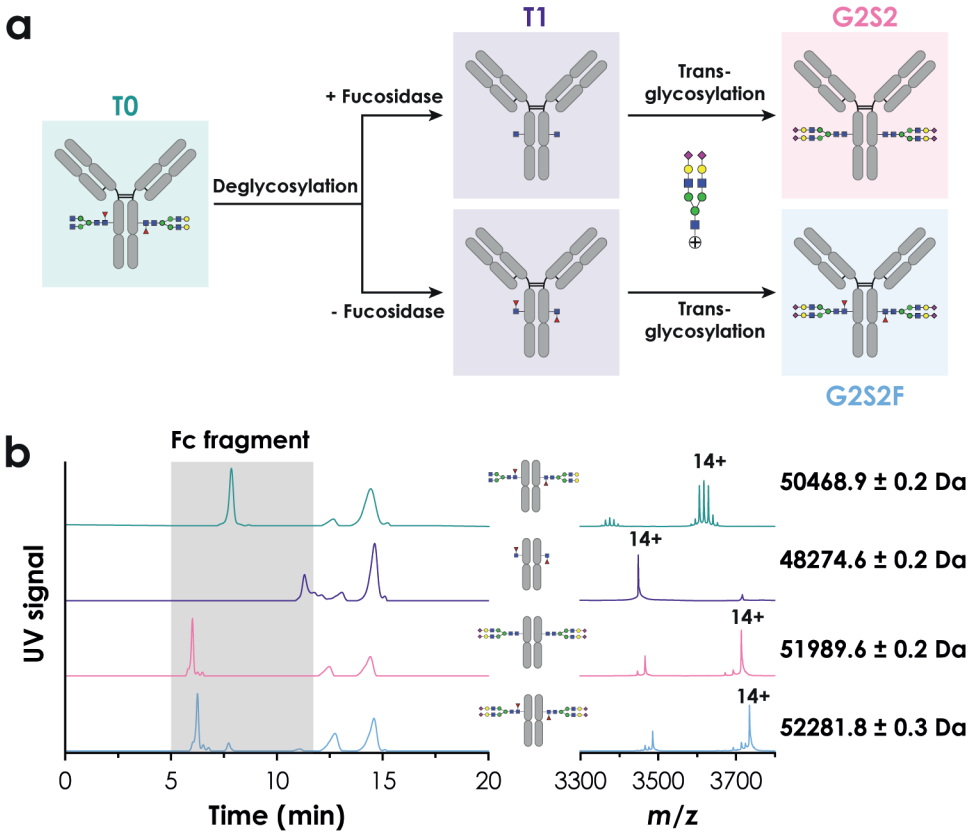

Figure 4 | Modification of the glycan moiety of trastuzumab. (**a**) Schematic overview of the glycan remodeling workflow. The deglycosylation was performed with or without presence of a fucosidase resulting in different starting points for the transglycosylation (either GlcNAcFuc or GlcNAc). (**b**) CEX-UV separation of glycoengineered trastuzumab at middle level highlighting the retention mass shift of the Fc domains. Corresponding mass spectra of the different Fc subunits including the (major) experimental mass are presented. Mass spectra of the $F(ab')_2$ domain can be found in **Figure S10**.

glycans showed a shift to lower retention times in CEX, specifically 6.0 min for G2S2 and 6.3 min for G2S2F compared to 8.0 min for T0 (**Fig. 4b**). Notably, the Fc fragment carrying G2S2F showed a minor peak around 9.8 min indicating that the reaction was not complete and a minor amount of the T0 product was still present. However, due to the CEX baseline separation of the different Fc fragments, there was no inference of these species in the region where the CIU fingerprints were recorded. The peaks of the $F(ab')_2$ fragment eluted at the same retention time (14.5 min) for all samples and showed similar mass spectra suggesting no other modifications is induced on this part during the sample treatment as expected (**Fig. S10**).

Comparing the CIU fingerprints of the glycosylated T0 product and the deglycosylated T1 product revealed the same number of transitions. Nevertheless, some differences can be observed regarding the gas-phase kinetic stability of the unfolding features of both subunits. For instance, the most unfolded conformation of T0 (12 ms) is the most populated conformation at 110 V whereas for T1, this conformation undergoes transition at lower collision energies and thus, the conformation observed at 10 ms is the most populated state at 110 V (**Fig. 5b**, and **c**). This indicates that deglycosylation of trastuzumab results in an Fc domain more prone to gas-phase unfolding, which is in agreement with previously performed differential scanning calorimetry (DSC) as well as CIU experiments [135, 256, 268, 269]. Regarding the CIU fingerprints of sialylated Fc variants, differential features can be also detected upon inspection of the unfolding patterns. Interestingly, an intermediate unfolding transition can be observed around 52 V for the G2S2, and G2S2F products, which was not observed for T0 or T1 (**Fig. 5a** and **c**). Furthermore, the most unfolded conformation of those products (state 3) was still detected as the most intense conformation at the highest voltage (130 V). These results clearly pinpoint that the presence of sialic acid glycans confers higher unfolding resistance to the Fc domain of the mAb. According to our results, the presence of core fucoses on these glycans does not influence the gas-phase unfolding mechanism of these products reflected in very similar unfolding patterns. The latter was also confirmed by previously reported DSC data, where afucosylated IgG1 glycoforms did not show different thermal unfolding compared to the fucosylated counterpart [270, 271]. Overall, the differences between glycan-remodeled Fc subunits were highlighted when performing differential analysis between the fingerprints (**Fig. S11**). Upon pairwise comparison, RMSD values greater than 14% were obtained (excluding the comparison between G2S2, and G2S2F, where almost no differences were observed), while the variation of the technical replicates was lower than 6%. According to the UFS plot, the most diagnostic voltages to

differentiate the glycoengineered Fc domains were between 100 V and 120 V (**Fig. S11c**, and **5b**). In addition, the Fc CIU features showed differences in the 20-60 V range. The extracted arrival time distributions (ATDs) at 40 V (**Fig. 5d**) revealed clear-cut differences between the glyco-engineered Fc domains compared to T0 and T1, with a different number of co-existing populations along with different relative intensities, allowing the categorization of the Fc species. As above mentioned, the presence of fucose does not significantly alter the Fc gas-phase unfolding mechanism thus, the high similarity of G2S2, and G2S2F ATDs profiles.

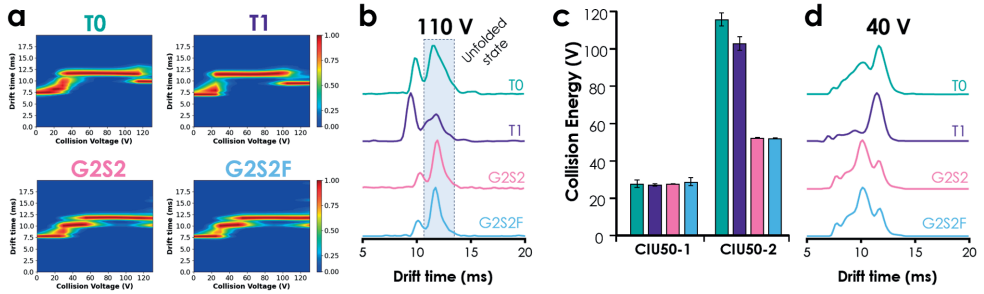

Figure 5 | CEX-CIU experiments of middle level of trastuzumab samples subjected to glycan-remodeling. (**a**) CIU fingerprints of the 14+ charge state of the Fc fragments carrying different glycans, including initial (T0, green), deglycosylated (T1, purple) and end (G2S2F, pink and G2S2, blue) products. Differential plots including RMSD values can be found in **Figure S11**. (**b**) ATDs extracted at 110 V evidencing the higher relative intensity of the most unfolded conformation in the case of G2S2, and G2S2F showing greater resistance to unfolding events. (**c**) CIU50 analysis of the samples revealing an intermediate transition only observed in the case of sialylated variants. (**d**) ATDs extracted at 40 V showing that differences in the ATD profile can also be detected in the low energy range of the CIU fingerprints. The $F(ab')_2$ CIU fingerprints showed no differences in resistance to gas-phase unfolding (**Fig. S12**).

The CIU patterns of the $F(ab')_2$ subunits revealed the same number of unfolding transitions along with very similar CIU50 values. The CIU patterns of the $F(ab')_2$ subunits revealed the same number of unfolding transitions along with very similar CIU50 values. Upon pairwise comparison of the $F(ab')_2$ fingerprints, the RMSD values were close to those obtained upon technical replicates which evidenced the similarities between the CIU fingerprints of those domains suggesting that the $F(ab')_2$ unfolding mechanism was not affected by the Fc glycan scaffold (**Fig. S12**). The same conclusion was upon technical replicates which evidenced the similarities drawn in previous studies based on DSC measurements, demonstrating that the melting temperatures of the Fab and CH3 domains of different N-glycosylated mAbs were not affected by the presence of different glycan moieties [272]. Altogether, the CEX-CIU approach was perfectly adapted to monitor structural modifications of mAbs, while simultaneously obtaining information on the unfolding mechanism of the chromatographically-selected species. The proposed experimental

set-up allowed the correlation between glycan-engineered scaffold and unfolding signatures in the CIU fingerprints providing valuable information on the influence of local structure alteration (i.e., altered glycan moieties) on the unfolding pattern of the Fc subunit of trastuzumab.

5.4 Conclusion

In this study, we aimed at the innovative hyphenation of CEX with CIU experiments to provide a thorough characterization of therapeutic proteins. This experimental set-up combined the benefits of CEX separation to afford information about protein heterogeneity together with the CIU analysis to allow the characterization of those protein populations beyond their folded state. After developing this approach at both intact and middle level, we showed that the analytical strategy is well-suited to record the global conformation and the CIU unfolding pattern of different CEX-separated species without affecting the resolution and chromatography separation capabilities, Moreover, the recorded CEX-CIU fingerprints contained a similar level of information compared to those obtained under classical ESI-CIU conditions.

To show the applicability of our innovative CEX-CIU platform, we focused on a mixture of three therapeutic mAbs close in mass but with different pIs and representatives from different subclasses (with different inter-chain disulfide patterns). The three CIU fingerprints exhibited different unfolding transitions leading to the conclusion that CEX-CIU was able to maintain the key features of the unfolding mechanism of each mAb and thus allowing the differentiation of those proteins. Furthermore, these results showed that the overall CEX-CIU analysis time could be significantly reduced when dealing with therapeutic mAb mixtures. Additionally, CEX-CIU coupling emerged as an appealing alternative in the particular case of isobaric mAb mixtures since these proteins cannot be separated using SEC-CIU. In this case, CEX-CIU affords a baseline-resolved separation according to mAb pIs, hence, CEX-CIU combines the synergy of separation based on pI and CIU recording.

Besides, applicability of CEX-CIU to obtain glycan-variant-specific information was investigated by studying the gas-phase unfolding of Fc regions carrying different glycan moieties. The Fc CIU patterns showed variations in gas-phase conformational transitions as a result of altered glycosylation, while conventional IM-MS measurements were unable to provide clear conclusions highlighting the suitability of CIU approach to study protein populations with similar CCS values. Based on the CIU patterns, it was shown that deglycosylated Fc fragments were more prone to unfolding events while

remodeled glycoforms showed increased resistance to gas-phase unfolding.

Altogether, the results provided in this study evidence that hyphenation of CEX with CIU has potential to provide in-depth characterization of therapeutic mAbs. First, CEX-CIU affords practical benefits, such as automation of CIU fingerprint recording while keeping pI separation without any prior sample preparation, leading to an increased throughput. More importantly, CEX-CIU not only enabled the identification of protein populations using classical CEX-nMS conditions but also offers the possibility of simultaneous conformational characterization of those chromatography-resolved populations. In future, the application of this approach could be further expanded to low abundant charge variant analysis, including deamidation and oxidation, either in drug products or in forced degraded samples. Both the level of structural information along with the streamlined analysis afforded by CEX-CIU approach make this technique particularly interesting to be integrated into R&D laboratories performing analysis of mAb-derived proteins.

Acknowledgments

This work was supported by the Netherlands Organization for Scientific Research NWO (SATIN project, Grant No. 731.017.202), the CNRS, the University of Strasbourg, the "Agence Nationale de la Recherche", and the French Proteomic Infrastructure (ProFI; ANR-10-INBS-08-03). The authors would like to thank GIS IBiSA and Région Grand Est for financial support in purchasing a Synapt G2 HDMS instrument. OHA acknowledges the "Agence Nationale de la Recherche" for funding his JCJC project "ConformAbs" (ANR-21-CE29-0009-01). J.C. acknowledges ANRT and NovaliX for funding of his PhD.

Supplementary information

The following supplementary files are available on request:

Influence of cone voltages on middle-level analysis (**Fig. S1**), CEX-CIU fingerprints with 4 or 6 IM-MS functions (**Fig. S2**), Effect order of applied CVs during peak elution (**Fig. S3**), CEX-CIU of middle-level trastuzumab (**Fig. S4**); Individual mass spectra and ATDs at different energies of Fc subunit (**Fig. S5**), Comparison ESI-CIU and CEX-ESI-CIU experiments (**Fig. S6**), CIU50 analysis of multiplexed mAbs (27+) (**Fig. S7**), CIU fingerprints and CIU50 analysis of multiplexed mAbs (26+) (**Fig. S8**), CIU fingerprints and CIU50 analysis of multiplexed mAbs (28+) (**Fig. S9**), Mass spectra $F(ab')_2$ fragments before and after glycan remodeling (**Fig. S10**), RMSD plots of Fc fragments with remodeled glycosylation (**Fig. S11**), CEX-CIU fingerprints of $F(ab')_2$ domains before and after glycan remodeling (**Fig. S12**), IM-nMS analysis of Fc domains with differences in glycosylation (**Fig. S13**), Retention times and relative peak areas of CEX separation (**Table S1**), Characteristics of multiplexed mAbs (**Table S2**).

5